Covalent Superlattice Structures at Silicon (111) Surfaces

J. E. Rowe and J. C. Phillips
Bell Laboratories, Murray Hill, New Jersey 07974
(Received 28 January 1974)

Low-energy electron-diffraction and photoemission data are presented for Si(111) surfaces with 2×1 and 7×7 superlattices, as well as for the disordered surface obtained in the transition from one to the other. Together with work-function measurements these data suggest two different models for the two superlattices.

Semiconductor surfaces exhibit superlattice structures which have been previously observed and discussed by many authors.[1-9] Most recent discussions[2-9] favor the *same mechanism* for all superlattices, with surface atoms displaced periodically leaving a buckled or rumpled surface, first proposed by Haneman.[5] In principle, these superlattices can be accurately analyzed from low-energy electron-diffraction (LEED) intensity theory and experiments. However, recent difficulties with the structures for chalcogens on Ni(100) surfaces[10] and with the Si(100) superlattice[11] indicate that further theoretical refinements are necessary before this approach can yield unique structural information.

In this Letter LEED and photoemission data are presented for cleaved and for annealed Si(111) surfaces with 2×1 and 7×7 superlattices, respectively, as well as for the surface (sometimes referred to as 1×1) obtained in the phase transition between the two superlattices which takes place near 400°C. *Two different models* for the two superlattices are necessary to explain the qualitatively large changes observed in LEED intensities and photoemission energy distributions in the transition 2×1 → 7×7.

LEED patterns for these three structures are shown in Fig. 1 at 60 eV electron energy. The surfaces were obtained by cleavage in ultrahigh vacuum[12] ($p < 10^{-10}$ Torr) [Fig. 1(a)] with subsequent annealing to 380 ± 20°C [Fig. 1(b)] and 700 ± 20°C [Fig. 1(c)]. Although the superlattice features are obviously quite different for the 2×1 and 7×7 structures, the integral-order beam intensities for both exhibit a sixfold symmetry which is the same as for hexagonal (111) planes of the bulk lattice. However, the integral-order beams in the transition structure have only a threefold symmetry, and the superlattice LEED features are replaced by an increased diffuse background intensity with some streaks near the integral-order beams, indicating short-range order similar to the 7×7 structure. Thus the transition structure involves disordering the 2×1 superlattice and we interpret the symmetry change, sixfold to threefold, as due to a change in the relative contributions of the top and second layers to the diffraction pattern. The (0001) graphite surface has a similar change in LEED symmetry with change in electron penetration depth.[13]

Recent data[7-9] for the temperature dependence of the work function is reproduced in Fig. 2. Similar to the LEED results the transition structure exhibits a large departure from the two ordered

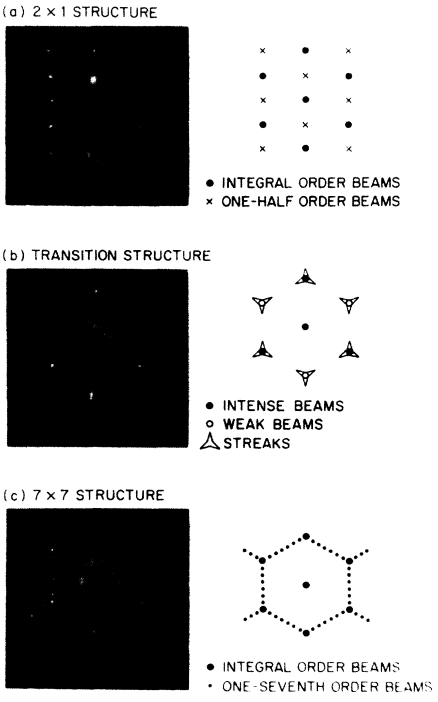

FIG. 1. Low-energy electron-diffraction patterns for the three surface structures indicated, taken at a primary energy of 60 eV. Note the change in the symmetry of the integral-order beams from sixfold to threefold for the transition structure.

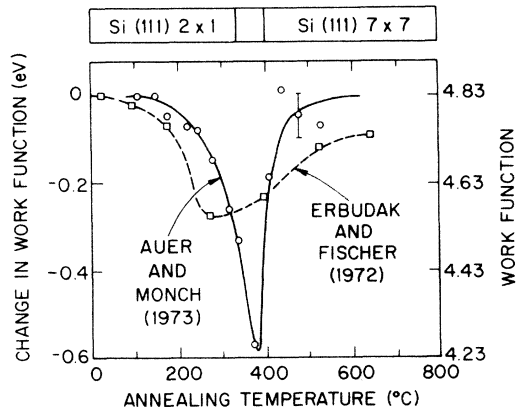

FIG. 2. The change in work function versus annealing temperature for silicon (111) surfaces as measured by Auer and Mönch (Ref. 7) and by Erbudak and Fischer (Ref. 8). The solid line is an empirical fit using an exponential activation function ($E_a = 0.63$ eV) and Lorentzian-broadened step-function cutoff of 410°C. Other data (Ref. 7), not shown, indicate that above 600°C, $\Delta\varphi$ levels off at -0.23 eV.

structures, indicating that two different mechanisms are responsible for the 2×1 and 7×7 superlattices. Thus while the displaced-atom model[1,5,6,14] appears to be a satisfactory explanation of the cleaved 2×1 surface, a qualitatively different model such as the surface-vacancy model first proposed by Lander[14] seems to be necessary for the annealed 7×7 surface. The work-function data can be fitted quite well, as the full line indicates, with an exponential activation function with an activation energy of 0.63 eV, cut off at $T_c = 410$°C, and broadened (Lorentzian half width at half-maximum $\Gamma = 18$°C). This fit shows that in the absence of broadening (which may be caused by surface steps) the maximum drop $\Delta\varphi_{max}$ at T_c would be about 1.2 eV.

For the transition structure, φ is decreasing with increasing temperature as vacancies are created and remain near steps. Vacancies at steps "round off" the step edge, weaken covalency, and cause the bonding between the planes to be more metallic. It has been shown[7] that for high step densities the transition temperature is proportional to the step density, which we believe to be the result of larger vacancy concentrations at higher step densities. When φ increases again the vacancies have begun to order by forming domains with 7×7 unit cells and with 28% of the atomic sites in the outer plane vacant. The restoration of covalent networks (now involving twelvefold as well as sixfold warped rings) returns the 7×7 φ to 0.23 eV below the 2×1 value. The reduction $\Delta\varphi_{max}$ of the work function as the (111) 2×1 surface is disordered contains a contribution of about 0.2 eV from the effects of band bending.[9] This leaves a large structural contribution $\Delta\varphi_s$, of order 1.0 eV, to be explained.

According to a model[15] previously developed to analyze heats of formation of bulk vacancies, dangling-bond energies can be separated into two parts, a larger metallic part, and a residual covalent part which is lost when the semiconductor, under pressure, transforms to the (metallic) white-Sn state. Thus, it is the presence or absence of the covalent surface network that is crucial to large-scale variations of the work function. The largest change in φ will take place if covalency is completely destroyed in the transition state, leaving only the metallic contribution to φ, a contribution which depends almost entirely on the valence electron density only.[16,17] We know, however, that Al and Si have nearly the same valence electron density; thus

$$\Delta\varphi_{max} = \varphi_{Al}(\text{polycryst}) - \varphi_{Si}(111)$$
$$= 4.22 - 4.83 = -0.6 \pm 0.1 \text{ eV}, \quad (1)$$

based on experimental values for Al[17] and Si[8] most-stable surfaces and neglecting the small Al anisotropy.[17]

Internal-reflection studies of the 2×1 surfaces have indicated[18] a band gap of $2\Delta = 0.26$ eV in the surface bands lying between the valence and conduction band edges. The contribution of this [Fermi surface (FS)] gap to the cohesive energy and hence to $\Delta\varphi_{max}$ can be estimated from phase-space considerations[19] to be

$$\Delta\varphi_{max}(\text{FS}) = \Delta^2/4W, \quad (2)$$

where W, the bandwidth of the surface bands, is[9] of order 1 eV. Thus Eq. (2) gives $\Delta\varphi_{max}(\text{FS}) \approx \Delta\varphi/100$, and the Fermi-surface[20] or Jahn-Teller mechanism[21] cannot explain the Si(7×7) superlattice.

Additional evidence for two different superlattice mechanisms (corresponding to the data of Figs. 1 and 2) comes from ultraviolet photoemission spectroscopy (UPS). In Fig. 3 we show UPS data at a photon energy of 21.2 eV, with the estimated bulk contribution[22] indicated as shaded areas. The upper part of the valence band (from 0 to -5 eV on the scale of Fig. 3) results from the long-range overlap of second- and higher-order neighbors similar to π electrons in a hydrocarbon-ring molecule. In a nearest-neighbor

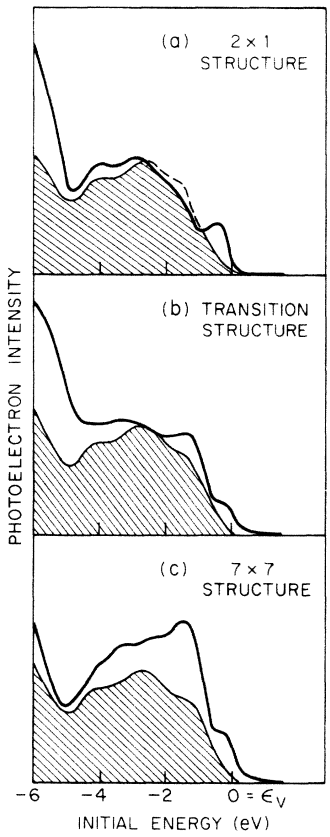

FIG. 3. Ultraviolet photoemission energy distribution curves at a photon energy of 21.2 eV for the three surface structures of Figs. 1 and 2. The energy zero is taken at the top of the bulk valence band and the estimated bulk contribution for each energy distribution curve is shown as a shaded area.

tight-binding model of silicon this contribution to the density of states appears as a delta-function peak.[23,24] Thus the results of Fig. 3 indicate the following: (a) For 2×1 structure the upper valence band is essentially bulklike except for the "dangling-bond" surface states near −0.5 eV. (b) For transition structure the "dangling-bond" surface states have shifted from −0.5 to 0.0 eV. In addition, new surface states appear at −1.5 and −3.6 eV indicating a change in the π-like electrons near the surface upon annealing.[25] (c) For 7×7 structure the additional surface features are now much more intense indicating the completion of a new covalent network at the surface. The increased intensity in the π-electron region arises from the larger polarizability of the twelvefold rings present in the Lander model compared to the sixfold (warped benzene) rings which dominate pairs of (111) bulk lattice planes. This increase is well established for conjugated hydrocarbons where it is described as polarizability exaltation.[26]

Although the evidence is not yet conclusive the discussion above is strongly indicative of the two separate structures, i.e., the Haneman model for the 2×1 and the Lander vacancy model for the 7×7 surface. Other experimental evidence which supports these conclusions includes (1) different behavior of LEED symmetry due to atomic H adsorption,[27] (2) patchiness of emission observed by ion neutralization spectroscopy,[28] (3) shifts of surface-state peaks (see Fig. 3) which are much larger than shifts in bulk band structure going from zinc blende to wurtzite,[29] and (4) observation of a 7×7 LEED pattern after room-temperature cleavage at a fault plane.[30] Thus the accumulation of a variety of data supports the conclusions of an earlier thermochemical analysis[31] which rejected the buckled model of annealed covalent surfaces.

The authors are grateful to Dr. H. Ibach for several stimulating discussions and for assisting with several experiments.

[1]J. J. Lander, G. W. Gobeli, and J. Morrison, J. Appl. Phys. 34, 2298 (1963).

[2]P. W. Palmberg and W. T. Peria, Surface Sci. 6, 57 (1967).

[3]G. A. Somorjai, Advan. Chem. Phys. 20, 215 (1971).

[4]S. G. Davidson and J. D. Levine, Solid State Phys. 25, 111 (1970).

[5]D. Haneman, Phys. Rev. 121, 1093 (1961); S. E. Trullinger and S. L. Cunningham, Phys. Rev. B 8, 2622 (1973).

[6]D. Haneman, W. D. Roots, and J. T. P. Grant, J. Appl. Phys. 38, 2203 (1967).

[7]P. P. Auer and W. Mönch, in Proceedings of the Second International Conference on Solid Surfaces, Kyoto, Japan, 25–29 March 1974 (to be published).

[8]M. Erbudak and T. E. Fischer, Phys. Rev. Lett. 29, 732 (1972).

[9]W. Mönch, in *Festkörperprobleme*, edited by H.-J. Queisser (Vieweg, Braunschweig, Germany, 1973), Vol. 13, p. 252.

[10]J. E. Demuth, D. W. Jepsen, and P. M. Marcus, Phys. Rev. Lett. 31, 540 (1973); S. Andersson, B. Kasemo, J. B. Pendry, and M. A. Van Hove, Phys. Rev. Lett. 31, 595 (1973); C. B. Duke, N. O. Lipari, G. E. Laramore, and J. B. Theeten, Solid State Commun. 13, 579 (1973).

[11]P. M. Marcus, D. W. Jepsen, and F. Jona, private communication.

[12]J. E. Rowe and H. Ibach, Phys. Rev. Lett. 31, 102 (1973); J. E. Rowe, S. B. Christman, and E. E. Chaban, Rev. Sci. Instrum. 44, 1675 (1973).

[13]G. Albinet, J. P. Biberian, and M. Bienfait, Phys.

Rev. B 3, 2015 (1971).
[14]J. J. Lander, in *Progress in Solid State Chemistry*, edited by H. Reiss (Pergamon, Oxford, England, 1965), Vol. 2, p. 26.
[15]J. C. Phillips and J. A. Van Vechten, Phys. Rev. Lett. 30, 220 (1973).
[16]J. Schmit and A. A. Lucas, Solid State Commun. 11, 415 (1972).
[17]J. C. Riviere, *Solid State Surface Science*, edited by M. Green (Marcel Dekker, New York, 1969), Vol. 1; N. D. Lang and W. Kohn, Phys. Rev. B 3, 1215 (1971).
[18]G. Chiarotti *et al.*, Phys. Rev. B 4, 3398 (1971).
[19]D. Penn, Phys. Rev. 128, 2093 (1962).
[20]L. Dobrzynski and D. C. Mills, Phys. Rev. B 7, 2367 (1973).
[21]P. Ducros, Surface Sci. 10, 295 (1968).
[22]J. E. Rowe and H. Ibach, Phys. Rev. Lett. 32, 421 (1974).
[23]S. G. Davison and J. D. Levine, Solid State Phys. 25, 2 (1970); D. Weaire and M. F. Thorpe, Phys. Rev. B 4, 2508 (1971).
[24]The π characteristics of the upper-valence-band charge distribution in Si are discussed by J. C. Phillips, *Bonds and Bands in Semiconductors* (Academic, New York, 1973), p. 145.
[25]The appearance of such structure below the top of the valence band can be associated with a contraction of the first and second atomic layers and associated modification of charge density. J. A. Appelbaum and D. R. Hamann, Phys. Rev. Lett. 31, 106 (1973).
[26]P. L. Davies, Trans. Faraday Soc. 48, 789 (1952).
[27]H. Ibach and J. E. Rowe, to be published.
[28]H. D. Hagstrum and G. E. Becker, Phys. Rev. B 8, 1592 (1973).
[29]M. Cardona and G. Harbeke, Phys. Rev. 137, A1467 (1965).
[30]G. Boskovitz and D. Haneman, Bull. Amer. Phys. Soc. 18, 298 (1973); J. W. T. Ridway and D. Haneman, Appl. Phys. Lett. 17, 130 (1970).
[31]J. C. Phillips, Surface Sci. 40, 459 (1973).

Heat Capacity and Metal-Insulator Transitions in Ti_4O_7 Single Crystals

C. Schlenker, S. Lakkis, and J. M. D. Coey
Groupe des Transitions de Phases, Centre National de la Recherche Scientifique, 38 042 Grenoble-Cedex, France

and

M. Marezio
Laboratoire des Rayons X, Centre National de la Recherche Scientifique, 38 042 Grenoble-Cedex, France
(Received 14 February 1974)

Heat-capacity and entropy changes at the metal-insulator transitions have been measured on Ti_4O_7 single crystals. The 130-K transition is related to a disordering of the Ti^{3+} and Ti^{4+} chains at the unit cell level. Ti^{3+} pairing occurs in this phase but without any long-range order of the bonds. It is shown from both magnetic-susceptibility and specific-heat data that for the 150-K transition, the electronic contribution seems to be of the same order of magnitude as the lattice contribution.

Titanium oxide Ti_4O_7 belongs to the class of materials which show metal-insulator transitions and have attracted considerable attention during the last decade.[1,2] It is one of the Magnéli phases Ti_nO_{2n-1} and is triclinic with two molecules per primitive cell.[3] The structure contains two types of Ti chains, running parallel to the pseudorutile c axis and truncated every four Ti by the crystallographic shear planes.[4] Ti_4O_7 exhibits two electrical transitions, a semiconductor-semiconductor transition at about 130 K and a semiconductor-metal one at about 150 K.[5] For both transitions, there is a steep increase of the electrical conductivity with increasing temperatures. The magnetic susceptibility shows a sharp enhancement at 150 K; it is small and temperature independent both below and above 150 K and does not show any anomaly at 130 K.[6] Marezio *et al.* showed that, below 130 K, the Ti chains are either Ti^{3+} or Ti^{4+} and that the 3+ sites are paired to form nonmagnetic Ti^{3+}-Ti^{3+} bonds [Figs. 3(a) and 3(b)]. Between 130 and 150 K, the crystal structure was found to be only slightly different from the room-temperature one.[4]

It was proposed that the low-temperature phase ($T < 130$ K) is insulating because of the localization of $3d$ electrons into nonmagnetic Ti^{3+}-Ti^{3+} bonds. The high-temperature phase ($T > 150$ K) is metallic because of the delocalization of the $3d$ electrons. The nature of the intermediate phase ($130 < T < 150$ K) is not clear. It has been suggested that there could be charge localization

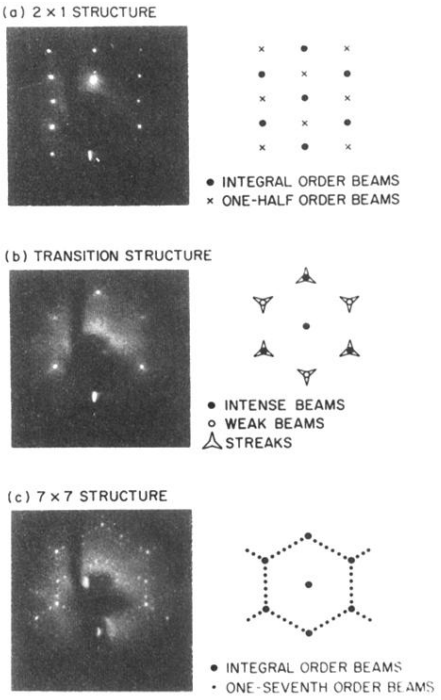

FIG. 1. Low-energy electron-diffraction patterns for the three surface structures indicated, taken at a primary energy of 60 eV. Note the change in the symmetry of the integral-order beams from sixfold to threefold for the transition structure.